Robust optimization to reduce the impact of biological effect variation from physical uncertainties in intensity-modulated proton therapy

Xuemin Bai[1], Gino Lim[1], David Grosshans[2], Radhe Mohan[3], Wenhua Cao[3,4]

[1] Department of Industrial Engineering, University of Houston, Houston, Texas, USA

[2] Department of Radiation Oncology, The University of Texas MD Anderson Cancer Center, Houston, Texas, USA

[3] Department of Radiation Physics, The University of Texas MD Anderson Cancer Center, Houston, Texas, USA

[4] Author to whom any correspondence should be addressed.

E-mail: wcao1@mdanderson.org

Abstract

Purpose: Robust optimization (RO) methods are applied to intensity-modulated proton therapy (IMPT) treatment plans to ensure their robustness in the face of treatment delivery uncertainties, such as proton range and patient setup errors. However, the impact of those uncertainties on the biological effect of protons has not been specifically considered. In this study, we added biological effect-based objectives into a conventional RO cost function for IMPT optimization to minimize the variation in biological effect.

Methods: One brain tumor case, one prostate tumor case and one head & neck tumor case were selected for this study. Three plans were generated for each case using three different optimization approaches: planning target volume (PTV)-based optimization, conventional RO, and RO incorporating biological effect (BioRO). In BioRO, the variation in biological effect caused by IMPT delivery uncertainties was minimized for voxels in both target volumes and critical structures, in addition to a conventional voxel-based worst-case RO objective function. The biological effect was approximated by the product of dose-averaged linear energy transfer (LET) and physical dose. All plans were normalized to give the same target dose coverage, assuming a constant relative biological effectiveness (RBE) of 1.1. Dose, biological effect, and their uncertainties were evaluated and compared among the three optimization approaches for each patient case.

Results: Compared with PTV-based plans, RO plans achieved more robust target dose coverage and reduced biological effect hot spots in critical structures near the target. Moreover, with their sustained robust dose distributions, BioRO plans not only reduced variations in biological effect in target and normal tissues but also further reduced biological effect hot spots in critical structures compared with RO plans.

Conclusion: Our findings indicate that IMPT could benefit from the use of conventional RO, which would reduce the biological effect in normal tissues and produce more robust dose distributions than those of PTV-based optimization. More importantly, this study provides a proof of concept that incorporating biological effect uncertainty gap into conventional RO would not only control the IMPT plan robustness in terms of physical dose and biological effect but also achieve further reduction of biological effect in normal tissues.

Keywords: IMPT, linear energy transfer, robust optimization, biological effect

1. Introduction

Proton beams have the ability to deposit dose over a confined distance at the end of the beam range, namely the Bragg peak, and almost no dose is released beyond the peak. This characteristic of proton beams provides an accurate localization of dose in three dimensions. As a result, intensity-modulated proton therapy (IMPT) delivered by pencil-beam scanning can generate highly conformal and homogeneous doses to target volumes with complex shapes while minimizing the undesired dose to adjacent organs at risk (OARs) (Lomax et al. 2001). However, proton beams are more sensitive to uncertainties that arise during treatment than are photon beams (Steneker, Lomax, and Schneider 2006). Indeed, in the most advanced form of IMPT, multifield optimized IMPT, the final dose distribution is obtained by superimposing all individual inhomogeneous proton fields, which may make IMPT even more sensitive to uncertainties than conventional proton modalities such as passive scattering proton therapy (PSPT) or single field uniform dose (SFUD) IMPT (Albertini et al. 2008). To address this issue of uncertainty, robust optimization (RO) is commonly used in IMPT treatment planning (Bangert, Hennig, and Oelfke 2013; Chen et al. 2012; Fredriksson, Forsgren, and Hårdemark 2011; Gordon et al. 2010; Lomax 2008b, 2008a; McGowan et al. 2015; Perkó et al. 2016; Pflugfelder, Wilkens, and Oelfke 2008; Unkelbach et al. 2009; Unkelbach, Chan, and Bortfeld 2007; Wahl et al. 2017).

The current practice of proton therapy uses a constant relative biological effectiveness (RBE) value of 1.1 to account for the biological effect of the treatment, as recommended by the International Commission on Radiation Units and Measurements (International Commission on Radiation Units and Measurements 2010). This value reflects the basic assumption that protons are 10% more biologically effective than photons. However, RBE varies along the treatment field, for instance with linear energy transfer (LET), tissue-specific parameters (defined by α and β), dose per fraction, and other factors (McNamara, Schuemann, and Paganetti 2015; Paganetti et al. 2002). The use of variable RBE in treatment planning is challenging because of considerable model uncertainties for clinical tissues,

because existing experimental biological data are insufficient to clearly correlate RBE and dose per fraction or $(\alpha/\beta)x$ for in vivo endpoints (Carabe et al. 2012; Giantsoudi et al. 2013; Paganetti et al. 2002; Resch et al. 2017). Moreover, treatment plans that use a variable RBE-weighted dose often deliver low physical doses in parts of the target because they assume that RBE is greater than 1.1 in areas of high LET (Paganetti 2014). On the other hand, if RBE is underestimated, critical structures may receive overdosage (Unkelbach et al. 2016).

Although factors such as tissue type, endpoint, and dose affect the relationship of RBE to LET, generally, biological effectiveness increases as LET increases (Carabe et al. 2013; Grassberger et al. 2011; McNamara, Schuemann, and Paganetti 2015; Polster et al. 2015; Wedenberg, Lind, and Hårdemark 2013). Unlike other biological parameters, LET can be calculated with high accuracy using analytical methods or Monte Carlo simulations (Cortés-Giraldo and Carabe 2015; Marsolat et al. 2016; Wilkens and Oelfke 2003). Previous studies have demonstrated that active scanning can shape the distribution of dose-averaged LET (i.e., the biological effect) without significantly altering the distribution of physical dose (Giantsoudi et al. 2013; Grassberger et al. 2011) because IMPT has a much higher degree of freedom for modulation than do other proton therapy modalities (Cao et al. 2018). Therefore, recent studies have attempted to optimize biological dose by simultaneously optimizing physical dose and LET distribution (An et al. 2017; Bassler et al. 2010; Cao et al. 2018; Fager et al. 2015; Giantsoudi et al. 2013; Grassberger et al. 2011; Inaniwa et al. 2017; Unkelbach et al. 2016). The primary focus of these studies was on increasing LET in radioresistant tumors or reducing it in critical normal tissues. However, the impact of IMPT delivery uncertainties on biological effect has not been carefully evaluated or included in optimization.

The aim of this work is to introduce a RO model for IMPT treatment plans that can achieve a robust biological effect distribution while maintaining satisfactory robust dose coverage in target volumes and sparing of critical structures. In the approach described here, the sum of the differences

between the highest and the lowest biological effect in each voxel, approximated by the product of dose and LET, was penalized to supplement a voxel-based worst-case RO cost function. This proof-of-concept study is demonstrated by IMPT treatment planning for three patient cases.

2. Methods and materials

2.1 Biological effect-based robust optimization (BioRO)

In IMPT, each beam consists of multiple beamlets that irradiate the tumor volume. The physical dose and LET delivered to voxel i by beamlet j in unit intensity are indicated as D_{ij} and L_{ij}. w_j^2 was used to denote the intensity of beamlet j to preserve the nonnegativity. Thus, for beamlet set N_B, the total dose D_i, dose-averaged LET L_i, and LET-weighted dose (LETxD) LD_i in voxel i can be calculated as follows:

$$D_i = \sum_j^{N_B} D_{ij} w_j^2 \tag{1}$$

$$L_i = \frac{\sum_j^{N_B} D_{ij} L_{ij} w_j^2}{\sum_j^{N_B} D_{ij} w_j^2} \tag{2}$$

$$LD_i = \sum_j^{N_B} D_{ij} L_{ij} w_j^2 \tag{3}$$

A research treatment planning platform, matRad (Wieser et al. 2017), was used to calculate D_{ij} and L_{ij} using a singular value decomposed pencil beam algorithm (Bortfeld, Schlegel, and Rhein 1993).

Commonly, IMPT uncertainties are handled by using margins. The clinical target volume (CTV) is expanded into the planning target volume (PTV), and planning is performed to irradiate the latter (Chen et al. 2012; Fredriksson, Forsgren, and Hårdemark 2011; Liu et al. 2012). For PTV-based optimization, a standard quadratic objective function is minimized as follows (Oelfke and Bortfeld 2001):

$$F_P(w_j) = p_T \frac{1}{N_T} \sum_{i=1}^{N_T} \left(D_i - D_{0,T}\right)^2 + p_{OAR} \frac{1}{N_{OAR}} \sum_{i=1}^{N_{ORA}} H\left(D_i - D_{0,OAR}\right) \times \left(D_i - D_{0,OAR}\right)^2 \tag{4}$$

where N_T, and N_{OAR} are sets of voxels in target volumes and OARs, respectively. Parameters p denote the penalty weights of the corresponding organs to control the priorities between competing objectives. D_0 terms are the prescribed doses required by the treatment plans. The heavy-side step function $H(D_i - D_{0,OAR})$ is a discontinuous function whose value is 0 for a nonpositive argument and 1 for a positive argument.

As alternatives to geometric margins, optimization methods that explicitly take setup and range uncertainties into account have been proposed (Fredriksson, Forsgren, and Hårdemark 2011; Liu et al. 2012; Lowe et al. 2017; Pflugfelder, Wilkens, and Oelfke 2008; Unkelbach et al. 2009). In these methods, dose distributions for multiple uncertainty scenarios are computed, and treatment plans are optimized with respect to all of the scenarios simultaneously. In this study, a voxel-based worst-case RO (Liu et al. 2012) method was used to penalize excessively high and low doses to target volumes and excessively high doses to OARs:

$$F_R(w_j) = p_{T,max}\frac{1}{N_T}\sum_{i=1}^{N_T}\left(D_{i,max} - D_{0,T}\right)^2 + p_{T,min}\frac{1}{N_T}\sum_{i=1}^{N_T}\left(D_{i,min} - D_{0,T}\right)^2 + p_{OAR}\frac{1}{N_{OAR}}\sum_{i=1}^{N_{ORA}} H\left(D_{i,max} - D_{0,OAR}\right) \times \left(D_{i,max} - D_{0,OAR}\right)^2 \quad (5)$$

Note that $D_{i,max} = \max_m\{D_i^m\}$ and $D_{i,min} = \min_m\{D_i^m\}$, $m \in M$, indicate the maximum and minimum dose, respectively, among nine ($|M|$=9) possible scenarios of voxel i, where m indicates uncertainty scenario and D_i^m indicate the dose calculation for voxel i in scenario m.

According to Unkelbach et al. (2016), the RBE-weighted dose b_i can be given using equation (6), where c is a scaling parameter set to 0.04 μm/keV. It consists of two components, a physical component (D_i) and a biological component (cLD_i). We consider the latter as an approximation of the biological effect from all incident proton fields for a given voxel. $LD_{i,max} = \max_m\{LD_i^m\}$ and $LD_{i,min} = \min_m\{LD_i^m\}$

denote the maximum and minimum LET-weighted dose, respectively, over all nine scenarios of voxel i, where LD_i^m indicate the product of dose and LET for voxel i in scenario m.

$$b_i = \sum_j^{N_B}\left(1 + cL_{ij}\right)D_{ij}w_j^2 = D_i + cLD_i \quad (6)$$

To reduce the variation in biological effect in each voxel i, we propose to add minimization of the uncertainty gap, i.e., $LD_{i,max} - LD_{i,min}$, into the conventional RO model. This approach follows the principles of info-gap decision theory (Ben-Haim 2006; Matrosov, Woods, and Harou 2013), which seeks to maximize the robustness of a decision given minimum performance requirements. In other words, only the robustness of biological effect is optimized; biological effect itself is not maximized or minimized in either target or normal tissues.

Therefore, we added the L2-norm of the uncertainty gap of biological effect to (5) to construct the quadratic objective function for the biological effect-based RO (BioRO):

$$F_B(w_j) = F_R(w_j) + p_{T,gap}\frac{1}{N_T}\sum_{i=1}^{N_T}\left(LD_{i,max} - LD_{i,min}\right)^2$$

$$+p_{OAR,gap}\frac{1}{N_{OAR}}\sum_{i=1}^{N_{OAR}}\left(LD_{i,max} - LD_{i,min}\right)^2 \quad (7)$$

In this study, PTV-based optimization, conventional RO, and BioRO models were solved by a quasi-Newton method, the limited-memory Broyden-Fletcher-Goldfarb-Shanno algorithm (Liu and Nocedal 1989). We implemented each of the models in our in-house IMPT treatment planning system (Cao et al. 2013; Cao et al. 2014). Calculations of dose and LET using unit beamlet intensity were performed using matRad, as mentioned earlier.

2.2 Patient cases and treatment planning

Three IMPT plans were generated to illustrate the PTV-based, RO, and BioRO methods for three clinical cases: a brain tumor case, a prostate tumor case and a head & neck tumor case (Table 1). For the brain tumor case, three sets of angle combinations (gantry and couch) were used: (260°, 10°), (100°, 350°), and (180°, 0°). Setup uncertainties of ± 3 mm in three dimensions and range uncertainties of ± 3.5% of the nominal range were assumed. Two beams, (90°, 0°) and (270°, 0°), were used for the prostate tumor case, with setup uncertainties of ± 5 mm and range uncertainties of ± 3.5% of the nominal range. Similarly, setup uncertainties of ±3 mm and range uncertainties of ± 3.5% of the beams' nominal range were assumed in the head and neck tumor case under three beams: (180°, 0°), (65°, 345°) and (300°, 20°). Therefore, both RO and BioRO considered nine scenarios, i.e., one nominal scenario (without the consideration of uncertainties), and eight uncertainty scenarios, including six setup uncertainty scenarios by shifting the patient's CT image (Albertini et al 2011) and two range uncertainty scenarios by scaling the nominal beamlet ranges (Schaffner and Pedroni 1998). The prescribed dose to target volumes and field arrangements were the same as those used in the clinical treatments. More planning details are listed in Table 1. The doses prescribed to all OARs were set to 0 in the optimizations.

Upon the completion of the optimization step for each of the three approaches, fixed RBE (1.1)-weighted dose (RWD) and LETxD were calculated for each of the nine scenarios. Note that each of the three plans was normalized to have 98% of the CTV covered by the prescribed dose. Dose-volume histograms (DVHs) and LETxD-volume histograms for the nominal scenario were used to quantify the plans' quality. To evaluate and compare the plan robustness, the envelope of all DVHs or LETxD-volume histograms in band graphs (Trofimov et al. 2010) and maps of the uncertainty gap for all nine scenarios were displayed. The difference between the worst and best value of a DVH point, such as $D_{v\%}$, is considered as the bandwidth at $D_{v\%}$ for a given organ.

3. Results

Figure 1 shows the DVH and LETxD volume histogram bands for the CTV and the brainstem for the three differently optimized IMPT plans in the brain tumor case. The DVH bands for the CTV were narrower for the RO and BioRO plans than for the PTV-based plan, indicating that the RO and BioRO plans were less sensitive to setup and range uncertainties than was the PTV-based plan. As we expected, the BioRO approach was able to generate robust physical dose distributions in the target volume that were comparable to those generated by the RO approach. Moreover, the DVH bands for the brainstem were similar for all three optimization techniques. We should note that the mean dose to the brainstem increased from 25.9 Gy with the RO plan to 27.8 Gy with the PTV-based plan and 28.3 Gy with the BioRO plan. However, the maximum dose to the brainstem was similar in all three plans; the maximum values (worst-case) of $D_{2\%}$ were 57.9 Gy, 54.5 Gy, and 54.8 Gy for the PTV-based, RO, and BioRO plans, respectively (Table 2).

In contrast, LETxD volume histogram bands of the three plans exhibited pronounced differences (Figure 1). The robustness of the LETxD distributions in both the CTV and the brainstem was markedly improved by the BioRO approach. For instance, the bandwidth at $D_{98\%}$ of c LETxD in the CTV was 0.4 Gy for the BioRO plan, 0.7 Gy for the PTV-based plan, and 0.5 Gy for the RO plan. The bandwidth at $D_{2\%}$ of c LETxD in the CTV was 0.7 Gy for the BioRO plan, but 2.0 Gy and 2.1 Gy for the PTV-based plan and the RO plan, respectively. Similarly, the bandwidth at $D_{2\%}$ of c LETxD in the brainstem was 0.7 Gy for the BioRO plan, smaller than the 2.6 Gy and 1.6 Gy bandwidths for the PTV-based and RO plans. The bandwidth at the mean value of c LETxD in the brainstem was also lower for the BioRO plan, 0.9 Gy compared to 2.6 Gy and 2.0 Gy for the PTV-based plan and the RO plan, respectively (Table 2).

The results for the prostate tumor case are shown in Figure 2 and Table 3. The differences in dose and LETxD distributions among the three IMPT plans were similar for the prostate and brain tumor cases. Note that the improvement in the robustness of LETxD with the BioRO plan in the bladder and rectum was modestly lower than in the brainstem as shown by the brain tumor case because of the

anatomy and the beam arrangement. The bandwidth at $D_{2\%}$ of c LETxD in the bladder was 1.7 Gy for the BioRO plan, smaller than the 3.8 Gy and 2.2 Gy bandwidths for the PTV-based plan and the RO plan, respectively (Table 3). The bandwidth at the mean value of c LETxD in the bladder was 0.4 Gy for the BioRO plan, 0.5 Gy for the PTV-based plan, and 0.7 Gy for the RO plan. In the rectum, the bandwidth at $D_{2\%}$ of c LETxD was 2.1 Gy for the BioRO plan, compared to 4.3 Gy and 2.4 Gy for the PTV-based plan and the RO plan, respectively. The bandwidth at the mean value of c LETxD in the rectum was 0.4 Gy for the BioRO plan, compared to 0.5 Gy and 0.9 Gy for the PTV-based plan and the RO plan.

The DVHs, c LETxD volume histograms and their statistics for the head and neck tumor case are shown in Figure A1, B1 and Table 4. The BioRO approach produced plan with more robust LETxD distribution than did the RO and PTV-based methods, and similar dose distribution compared to RO plan which is better than PTV-based plan. The bandwidth at $D_{2\%}$ of c LETxD in the larynx was 0.8 Gy for the BioRO plan, 2.1 Gy for the PTV-based plan, and 1.2 Gy for the RO plan. The bandwidth at the mean value of c LETxD in the larynx was 0.4 Gy for the BioRO plan, 0.8 Gy for the PTV-based plan, and 1.0 Gy for the RO plan. In the parotid (right), the bandwidth at $D_{2\%}$ of c LETxD was 0.8 Gy for the BioRO plan, smaller than the 1.5 Gy and 1.2 Gy bandwidths for the PTV-based and RO plans; and the bandwidth at mean value of c LETxD was 0.4 Gy for the BioRO plan, smaller than the 0.7 Gy and 0.6 Gy bandwidths for the PTV-based and RO plans. Similarly, the bandwidth at $D_{2\%}$ of c LETxD in the parotid (left) was 1.1 Gy for the BioRO plan compared to 1.3 Gy for the PTV plan and 2.2 Gy for the RO plan; the bandwidth at mean value of c LETxD in the parotid (left) was 0.2 Gy for the BioRO plan compared to 0.2 Gy for the PTV plan and 0.3 Gy for the RO plan.

Figure 3 shows uncertainty maps for the three plans for the brain tumor case. The RO method was the most robust in terms of physical dose distribution in the target and brainstem. Moreover, the RO plan was more robust than the PTV-based plan in terms of LETxD. The BioRO method, which minimized the variation in biological effect, led to a remarkable reduction of LETxD hot spots, especially

in the brainstem. Meanwhile, the robustness of the physical dose distribution for the BioRO plan was improved compared to the PTV-based plan.

As shown in Figure 4, the biological effect in the nominal scenario was the lowest for the BioRO plan, especially in critical organs. However, there was almost no difference among the three plans in the physical dose distributions for the nominal scenario (see subfigure (a-b), (a-c) and (b-c)).

4. Discussion

Three has been a growing interest in LET-based IMPT planning, including novel forward planning techniques and optimization methods(An et al. 2017; Bassler et al. 2010; Cao et al. 2018; Fager et al. 2015; Giantsoudi et al. 2013; Grassberger et al. 2011; Inaniwa et al. 2017; Unkelbach et al. 2016). The primary goal of LET-based planning is to place areas of higher LET to achieve a greater biological effect in radioresistant tumors while minimizing LET in critical structures to avoid unnecessary tissue damage. At the same time, LET-based planning keeps physical dose distributions as similar as possible to those currently used in proton therapy with fixed RBE planning. These methods have demonstrated the potential of increasing LET in target regions and/or reducing LET in normal tissues without excessively compromising current dose requirements. However, the challenge of IMPT delivery uncertainties has been largely ignored. The BioRO approach to IMPT planning proposed in the present study focuses on minimizing the variation in biological effect attributable to physical uncertainties for both target and normal tissues. The uncertainty gap minimization method was effective in reducing the spread of LETxD-volume histogram bands in this study. In other words, this approach could produce treatment plans with a high certainty of biological effect with satisfactory physical dose plan quality.

RO has been shown to deliver IMPT more safely than conventional PTV-based optimization (Fredriksson, Forsgren, and Hårdemark 2011; Liu et al. 2012; Lowe et al. 2017; Pflugfelder, Wilkens, and Oelfke 2008; Unkelbach et al. 2009). RO provides dose distributions that are robust against delivery

uncertainties, especially because it limits the impact of shifted Bragg peaks at the beam's distal edge, close to the target boundary. Therefore, researchers have proposed that unlike PTV-based plans, RO plans may alleviate increased LET or LETxD in OARs adjacent to the target (Giantsoudi et al. 2017). Our study confirmed that this is the case. For example, compared to the PTV-based plan, LETxD for 2% of the volume and mean LETxD for the brainstem were reduced by 15% and 11%, respectively, with RO. Similarly, LETxD for 2% of the volume and mean LETxD for the rectum were reduced by 33% and 43%, respectively.

Interestingly, the BioRO plan further reduced LETxD in OARs than the RO plan for both patient cases. For example, for the brain tumor case, compared to the PTV-based plan, LETxD for 2% of the volume and mean LETxD for the brainstem were reduced by 48% and 43%, respectively. Similarly, for the prostate tumor case, LETxD for 2% of the volume and mean LETxD for the rectum were reduced by 40% and 43%, respectively. This finding may be nonintuitive, as minimization of LETxD was not specified in the BioRO cost function. Instead, the uncertainty gap of LETxD was minimized. We conjecture that the reduction of LETxD in BioRO plans is attributable to the positive correlation between the uncertainty gap of LETxD and the nominal LETxD. For instance, a higher LETxD leads to a larger uncertainty gap, as either nominal LETxD or LETxD in various uncertainty scenarios is modulated by the same set of beamlet intensities, i.e., $LD_i = \sum_j^{N_B} D_{ij} L_{ij} w_j^2$. In all patient cases, we found that the sum of all beamlet intensities for the BioRO plan was the lowest among the three plans. However, these reduced total intensities did not necessarily lead to a cold plan in terms of dose, as seen in this study, because of the solution degeneracy of IMPT optimization.

We also note that our method is similar to ones proposed by Giantsoudi et al (2017) and An et al (2017) in which biological effect was included in the robust optimization framework. But our method is different in terms of its objectives that minimize the impact of physical uncertainties on biological effect,

i.e., those uncertainty gap terms, instead of minimizing worst-case biological effect. The difference among methods is worth investigating in future studies. Moreover, the information gap concept could also be applied in the robust optimization of dose, compared to the worse case optimization strategies extensively used in the literature. However, this may require a comprehensive comparison study and is beyond the scope of this paper concerning biological effect robustness.

Moreover, the BioRO plan also reduced LETxD in the target for all patient cases. However, the reduction in the target dose was much smaller than it was in OARs. The main reason for this difference may be that the BioRO plan enforced the requirement of prescribed dose to the target, but not to OARs, for which there was no lower dose limit. One straightforward method to avoid the reduction of LETxD in the target could be to use an additional objective to maximize the nominal or minimum LETxD for target voxels. Such a method for managing the trade-off between optimality and robustness with regard to biological effect needs to be explored in future research.

The gain in LET or LETxD while maintaining dose requirements is mainly achievable because IMPT provides a higher degree of freedom for optimization, i.e., intensity modulation. Our study demonstrated that plan robustness to biological effect can be improved by redistributing LETxD. Similarly, previous studies showed that LET and LETxD were improved by redistributing them (Cao et al. 2018; Inaniwa et al. 2017; Unkelbach et al. 2016). Because large uncertainties in proton RBE models remain a challenge to implementing RBE-based optimization in clinical practice, LET- or LETxD-based optimization is a promising method for improving the current proton treatment by moving toward biological effect-based IMPT planning.

5. Conclusion

We presented a proof-of-concept study of biological effect-based IMPT robust optimization in order to reduce the impact of variation in protons' biological effect while limiting the degradation of the physical dose distribution from a voxel-based worst-case RO plan. By minimizing the uncertainty gap of the biological effect (approximated by the product of LET and physical dose) in each voxel, the BioRO approach provided robust distributions of biological effect to both target and critical structures. This approach does not depend on tissue parameters or variable RBE models, which are associated with large uncertainties. In addition, our three patient case studies demonstrated that BioRO can avoid elevating biological effect in critical structures.

Acknowledgments

The authors would like to thank Dr. Amy Ninetto for her help editing this manuscript and Hans-Peter Wieser for his assistance with using matRad. This work was supported in part by the National Cancer Institute of the National Institutes of Health (2U19CA021239-35) and the Cancer Prevention and Research Institute of Texas (RP160232).

References

Albertini F, et al. 2008. “Sensitivity of Intensity Modulated Proton Therapy Plans to Changes in Patient Weight.” *Radiotherapy and Oncology* 86(2): 187–94.

Albertini F, Hug E B and Lomax A J. 2011. “Is It Necessary to Plan with Safety Margins for Actively Scanned Proton Therapy?” *Physics in Medicine & Biology* 56(14): 4399.

An Y, et al. 2017. “Robust Intensity-Modulated Proton Therapy to Reduce High Linear Energy Transfer in Organs at Risk.” *Medical Physics* 44(12): 6138–47.

Bangert M, Hennig P, and Oelfke U. 2013. “Analytical Probabilistic Modeling for Radiation Therapy Treatment Planning.” *Physics in Medicine and Biology* 58(16): 5401–19.

Bassler N, Jäkel O, Søndergaard CS, and Petersen JB. 2010. “Dose-and LET-Painting with Particle Therapy.” *Acta Oncologica* 49(7): 1170–76.

Ben-Haim Y. 2006. Academic Press *Info-Gap Decision Theory: Decisions Under Severe Uncertainty*. London: Academic Press.

Bortfeld T, Schlegel W, and Rhein B. 1993. “Decomposition of Pencil Beam Kernels for Fast Dose Calculations in Three-Dimensional Treatment Planning.” *Medical Physics* 20(2): 311–18.

Cao W, et al. 2013. “Incorporating deliverable monitor unit constraints into spot intensity optimization in intensity-modulated proton therapy treatment planning.” *Physics in Medicine and Biology* 58(15): 5113-25.

Cao W, et al. 2014. “Proton energy optimization and reduction for intensity-modulated proton therapy.” *Physics in Medicine and Biology* 59(21): 6341-54.

Cao W, et al. 2018. “Linear Energy Transfer Incorporated Intensity Modulated Proton Therapy Optimization.” *Physics in Medicine and Biology* 63(1): 15013.

Carabe A, et al. 2012. “Range Uncertainty in Proton Therapy Due to Variable Biological Effectiveness.” *Medical Physics* 57(5): 1159-72.

Carabe A, España S, Grassberger C, and Paganetti H. 2013. “Clinical Consequences of Relative Biological Effectiveness Variations in Proton Radiotherapy of the Prostate, Brain and Liver.” *Physics in Medicine and Biology* 58(7): 2103–17.

Chen W, et al. 2012. “Including Robustness in Multi-Criteria Optimization for Intensity-Modulated Proton Therapy.” *Physics in Medicine and Biology* 57(3): 591–608.

Cortés-Giraldo MA, and Carabe A. 2015. “A Critical Study of Different Monte Carlo Scoring Methods of Dose Average Linear-Energy-Transfer Maps Calculated in Voxelized Geometries Irradiated with Clinical Proton Beams.” *Physics in Medicine and Biology* 60(7): 2645–69.

Fager M, et al. 2015. “Linear Energy Transfer Painting with Proton Therapy: A Means of Reducing Radiation Doses with Equivalent Clinical Effectiveness.” *International Journal of Radiation Oncology Biology Physics* 91(5): 1057–64.

Fredriksson A, Forsgren A, and Hårdemark B. 2011. “Minimax Optimization for Handling Range and Setup Uncertainties in Proton Therapy.” *Medical Physics* 38(3): 1672–84.

Giantsoudi D, et al. 2017. “Can Robust Optimization for Range Uncertainty in Proton Therapy Act as a Surrogate for Biological Optimization?” *International Journal of Radiation Oncology, Biology, Physics* 99(2): S106–7.

342 Giantsoudi D, et al. 2013. “Linear Energy Transfer-Guided Optimization in Intensity Modulated Proton
343 Therapy: Feasibility Study and Clinical Potential.” *International Journal of Radiation Oncology*
344 *Biology Physics* 87(1): 216–22.

345 Gordon J J, et al. 2010. “Coverage Optimized Planning: Probabilistic Treatment Planning Based on Dose
346 Coverage Histogram Criteria.” *Medical Physics* 37(2): 550–63.

347 Grassberger C, Trofimov A, Lomax A, and Paganetti H. 2011. “Variations in Linear Energy Transfer within
348 Clinical Proton Therapy Fields and the Potential for Biological Treatment Planning.” *International*
349 *Journal of Radiation Oncology Biology Physics* 80(5): 1559–66.

350 Inaniwa T, Kanematsu N, Noda K, and Kamada T. 2017. “Treatment Planning of Intensity Modulated
351 Composite Particle Therapy with Dose and Linear Energy Transfer Optimization Treatment Planning
352 of Intensity Modulated Composite Particle Therapy with Dose and Linear Energy Transfer
353 Optimization.” *Physics in Medicine and Biology* 62(12): 5180–97.

354 International Commission on Radiation Units and Measurements. 2010. “Prescribing, Recording, and
355 Reporting Photon-Beam IMRT .” *Journal of the ICRU* 10(1): 7–16.

356 Liu DC, and Nocedal J. 1989. “On the Limited Memory BFGS Method for Large Scale Optimization.”
357 *Mathematical Programming* 45(1–3): 503–28.

358 Liu W, Zhang X, Li Y, and Mohan R. 2012. “Robust Optimization of Intensity Modulated Proton Therapy.”
359 *Medical Physics* 39(2): 1079–91.

360 Lomax AJ, et al. 2001. “Intensity Modulated Proton Therapy: A Clinical Example.” *Medical Physics* 28(3):
361 317–24.

Lomax AJ. 2008a. “Intensity Modulated Proton Therapy and Its Sensitivity to Treatment Uncertainties 1: The Potential Effects of Calculational Uncertainties.” *Physics in Medicine and Biology* 53(4): 1027–42.

Lomax AJ. 2008b. “Intensity Modulated Proton Therapy and Its Sensitivity to Treatment Uncertainties 2: The Potential Effects of Inter-Fraction and Inter-Field Motions.” *Physics in Medicine and Biology* 53(4): 1043–56.

Lowe M, et al. 2017. “A Robust Optimisation Approach Accounting for the Effect of Fractionation on Setup Uncertainties.” *Physics in Medicine and Biology* 62(20): 1–20.

Marsolat F, De Marzi L, Pouzoulet F, and Mazal A. 2016. “Analytical Linear Energy Transfer Model Including Secondary Particles: Calculations along the Central Axis of the Proton Pencil Beam.” *Physics in Medicine and Biology* 61(2): 740–57.

Matrosov ES, Woods AM, and Harou JJ. 2013. “Robust Decision Making and Info-Gap Decision Theory for Water Resource System Planning.” *Journal of Hydrology* 494: 43–58.

McGowan S E, Albertini F, Thomas S J, and Lomax A J. 2015. “Defining Robustness Protocols: A Method to Include and Evaluate Robustness in Clinical Plans.” *Physics in Medicine and Biology* 60(7): 2671–84.

McNamara AL, Schuemann J, and Paganetti H. 2015. “A Phenomenological Relative Biological Effectiveness (RBE) Model for Proton Therapy Based on All Published *in Vitro* Cell Survival Data.” *Physics in Medicine and Biology* 60(21): 8399–8416.

Oelfke U, and Bortfeld T. 2001. “Inverse Planning for Photon and Proton Beams.” *Medical Dosimetry* 26(2): 113–24.

Paganetti H, et al. 2002. “Relative Biological Effectiveness (RBE) Values for Proton Beam Therapy.” *International Journal of Radiation Oncology*Biology*Physics* 53(2): 407–21.

Paganetti H. 2014. “Relative Biological Effectiveness (RBE) Values for Proton Beam Therapy. Variations as a Function of Biological Endpoint, Dose, and Linear Energy Transfer.” *Physics in Medicine and Biology* 59(22): R419–72.

Perkó Z, et al. 2016. “Fast and Accurate Sensitivity Analysis of IMPT Treatment Plans Using Polynomial Chaos Expansion.” *Physics in Medicine and Biology* 61(12): 4646–64.

Pflugfelder D, Wilkens JJ, and Oelfke U. 2008. “Worst Case Optimization: A Method to Account for Uncertainties in the Optimization of Intensity Modulated Proton Therapy.” *Physics in Medicine and Biology* 53(6): 1689–1700.

Polster L, et al. 2015. “Extension of TOPAS for the Simulation of Proton Radiation Effects Considering Molecular and Cellular Endpoints.” *Physics in medicine and biology* 60(13): 5053–70.

Resch AF, et al. 2017. “Quantification of the Uncertainties of a Biological Model and Their Impact on Variable RBE Proton Treatment Plan Optimization.” Physica Medica 36: 91–102.

Schaffner, B, and E Pedroni. 1998. “The Precision of Proton Range Calculations in Proton Radiotherapy Treatment Planning: Experimental Verification of the Relation between CT-HU and Proton Stopping Power.” *Physics in Medicine and Biology* 43(6): 1579–92.

Steneker M, Lomax A, and Schneider U. 2006. “Intensity Modulated Photon and Proton Therapy for the Treatment of Head and Neck Tumors.” *Radiotherapy and Oncology* 80(2): 263–67.

Trofimov A, et al. 2010. " Evaluation of Dosimetric Gain and Uncertainties in Proton Therapy Delivery with Scanned Pencil Beam in Treatment of Base-of-Skull and Spinal Tumors. " *International Journal of Radiation Oncology*Biology*Physics* 78(3): S113–S114.

Unkelbach J, et al. 2016. “Reoptimization of Intensity Modulated Proton Therapy Plans Based on Linear Energy Transfer.” *International Journal of Radiation Oncology*Biology*Physics* 96(5): 1097–1106.

Unkelbach J, Bortfeld T, Martin BC, and Soukup M. 2009. “Reducing the Sensitivity of IMPT Treatment Plans to Setup Errors and Range Uncertainties via Probabilistic Treatment Planning.” *Medical Physics* 36(1): 149–63.

Unkelbach J, Chan TCY, and Bortfeld T. 2007. “Accounting for Range Uncertainties in the Optimization of Intensity Modulated Proton Therapy.” *Physics in Medicine and Biology* 52(10): 2755–73.

Wahl N, Hennig P,Wieser H P, and Bangert M. 2017. “Efficiency of Analytical and Sampling-Based Uncertainty Propagation in Intensity-Modulated Proton Therapy.” *Physics in Medicine & Biology* 62(14): 5790–5807.

Wedenberg M, Lind BK, and Hårdemark B. 2013. “A Model for the Relative Biological Effectiveness of Protons: The Tissue Specific Parameter α / β of Photons Is a Predictor for the Sensitivity to LET Changes.” *Acta Oncologica* 52(3): 580–88.

WieserHP, et al. 2017. “Development of the Open-Source Dose Calculation and Optimization Toolkit MatRad.” *Physics in Medicine and Biology* 44(6): 2556–68.

Wilkens JJ, and Oelfke U. 2003. “Analytical Linear Energy Transfer Calculations for Proton Therapy.” *Medical Physics* 30(5): 806–15.

426

427

Table 1. Patients information and treatment planning parameters.

Cancer type	Prescription dose (Gy/fx)	Number of fractions	Beam angles (gantry, couch)	Number of beamlets	Volumes included in optimization
Prostate	1.8 (CTV)	30	(90°, 0°)	5532	CTV, PTV, bladder, femoral heads, rectum
			(270°, 0°)	5525	
Brain	2 (CTV)	39	(260°, 10°)	3808	CTV, PTV, brainstem, optic chiasm, spinal cord, brain
			(100°, 350°)	3902	
			(180°, 0°)	3927	
H&N	2 (CTV)	33	(180°, 0°)	23758	CTV, PTV, left parotid, right parotid, larynx, spinal cord, mandible, left cochlea, right cochlea, brainstem, esophagus
			(65°, 345°)	25656	
			(300°, 20°)	25352	

Abbreviations: CTV, clinical target volume; PTV, planning target volume

Table 2. Dose and LET-weighted dose (LETxD; scaled by c = 0.04 µm/keV) values in the clinical target volume (CTV) and the brainstem for a brain tumor case optimized by PTV-based optimization, robust optimization (RO), and biological effect-based robust optimization (BioRO) approaches.

Tissue	**Dosimetric**	**PTV-based**			**RO**			**BioRO**		
	Parameter	Nom	Max	Min	Nom	Max	Min	Nom	Max	Min
CTV	$D_{98\%}$ (Gy[RBE])	54.0	55.0	49.6	54.0	54.4	51.4	54.0	54.8	51.3
	$D_{2\%}$ (Gy[RBE])	55.6	58.0	54.6	55.3	55.5	54.8	55.8	56.2	55.1
	c LETx$D_{98\%}$ (Gy)	3.6	4.0	3.3	4.4	4.5	4.0	3.6	3.8	3.4
	c LETx$D_{2\%}$ (Gy)	7.2	8.4	6.4	6.9	8.1	6.0	5.3	5.7	5.0
Brainstem	$D_{2\%}$ (Gy[RBE])	54.3	57.9	50.4	54.0	54.5	51.6	53.8	54. 8	51.2
	D_{mean} (Gy[RBE])	27.8	35.2	20.4	25.9	31.9	19.9	28.3	35.0	21.4
	c LETx$D_{2\%}$ (Gy)	9.4	10.2	7.6	8.0	8.6	7.0	4.9	5.3	4.6
	c LETxD_{mean} (Gy)	4.7	6.0	3.4	4.2	5.2	3.2	2.7	3.2	2.3

Abbreviations: RBE, relative biological effectiveness; Nom, nominal

Table 3. Dose and LET-weighted dose (LETxD; scaled by c = 0.04 µm/keV) values in the clinical target volume (CTV), rectum, and bladder for a prostate tumor case optimized using PTV-based optimization, robust optimization (RO), and biological-based robust optimization (BioRO) approaches.

Tissue	**Dosimetric Parameters**	**PTV-based**			**RO**			**BioRO**		
		Nom	Max	Min	Nom	Max	Min	Nom	Max	Min
CTV	$D_{98\%}$ (Gy[RBE])	78.0	80.0	68.2	78.0	78.8	73.5	78.0	78.7	73.5
	$D_{2\%}$ (Gy[RBE])	81.8	89.6	79.0	80.3	80.8	78.8	80.1	80.8	78.7
	c LETx$D_{98\%}$ (Gy)	3.6	5.2	2.8	5.0	5.5	4.5	4.5	4.9	4.0
	c LETx$D_{2\%}$ (Gy)	8.7	10.4	7.2	6.9	8.6	5.8	5.9	6.6	5.3
Rectum	$D_{2\%}$ (Gy[RBE])	72.0	81.2	49.7	71.9	78.4	51.1	71.7	78.2	52.1
	$D_{2\%}$ (Gy[RBE])	72.0	81.2	49.7	71.9	78.4	51.1	71.7	78.2	52.1
	c LETx$D_{2\%}$ (Gy)	5.8	8.2	3.9	3.9	5.0	2.6	3.5	4.4	2.3
	c LETxD_{mean} (Gy)	0.7	1.2	0.3	0.4	0.7	0.2	0.4	0.6	0.2
Bladder	$D_{2\%}$ (Gy[RBE])	78.4	84.1	63.7	73.3	78.4	61.6	73.6	78.3	62.3
	D_{mean} (Gy[RBE])	8.7	12.0	5.7	7.6	10.4	5.1	7.8	10.6	5.3
	c LETx$D_{2\%}$ (Gy)	8.7	9.9	6.1	6.6	7.6	5.4	5.4	6.1	4.4
	c LETxD_{mean} (Gy)	0.9	1.2	0.5	0.7	1.0	0.5	0.6	0.8	0.4

Abbreviations: RBE, relative biological effectiveness; Nom, nominal

Table 4. Dose and LET-weighted dose (LETxD; scaled by c = 0.04 µm/keV) values in the clinical target volume (CTV), larynx and parotid (right & left) for a H&N tumor case optimized using PTV-based optimization, robust optimization (RO), and biological-based robust optimization (BioRO) approaches.

Tissue	Dosimetric Parameters	PTV-based			RO			BioRO		
		Nom	Max	Min	Nom	Max	Min	Nom	Max	Min
CTV	$D_{98\%}$ (Gy[RBE])	66.0	67.0	63.8	66.0	66.5	64.5	66.0	66.5	64.9
	$D_{2\%}$ (Gy[RBE])	67.4	69.0	66.8	67.5	67.8	66.6	67.4	67.8	66.6
	c $LETxD_{98\%}$ (Gy)	3.7	3.9	3.5	3.8	4.0	3.6	3.6	3.8	3.4
	c $LETxD_{2\%}$ (Gy)	6.1	6.6	5.6	6.2	7.0	5.7	5.9	6.4	5.5
Larynx	$D_{2\%}$ (Gy[RBE])	66.5	69.3	64.5	65.6	66.4	63.8	65.4	66.2	63.6
	D_{mean} (Gy[RBE])	20.8	25.9	16.1	17.3	21.6	13.3	19.4	23.3	15.5
	c $LETxD_{2\%}$ (Gy)	6.9	7.9	5.8	6.1	6.5	5.3	4.8	5.1	4.3
	c $LETxD_{mean}$ (Gy)	2.0	2.5	1.5	1.5	2.0	1.2	1.4	1.6	1.2
Parotid_R	$D_{2\%}$ (Gy[RBE])	66.3	67.7	64.8	66.4	66.8	65.8	66.4	66.8	65.8
	D_{mean} (Gy[RBE])	16.5	19.9	13.3	13.8	16.7	11.1	15.1	18.1	12.2
	c $LETxD_{2\%}$ (Gy)	5.3	6.1	4.6	5.0	5.7	4.5	4.6	5.0	4.2
	c $LETxD_{mean}$ (Gy)	1.1	1.5	0.8	1.0	1.3	0.7	0.9	1.1	0.7
Parotid_L	D_{mean} (Gy[RBE])	37.6	44.4	31.4	30.8	38.5	23.0	30.0	36.4	23.1
	c $LETxD_{2\%}$ (Gy)	6.1	8.7	4.0	3.0	4.8	1.8	3.0	4.5	1.9
	c $LETxD_{mean}$ (Gy)	2.7	3.3	2.0	3.2	4.4	2.4	2.4	3.0	1.9
	c $LETxD_{mean}$ (Gy)	0.4	0.5	0.3	0.3	0.5	0.2	0.3	0.4	0.2

Abbreviations: RBE, relative biological effectiveness; Nom, nominal.

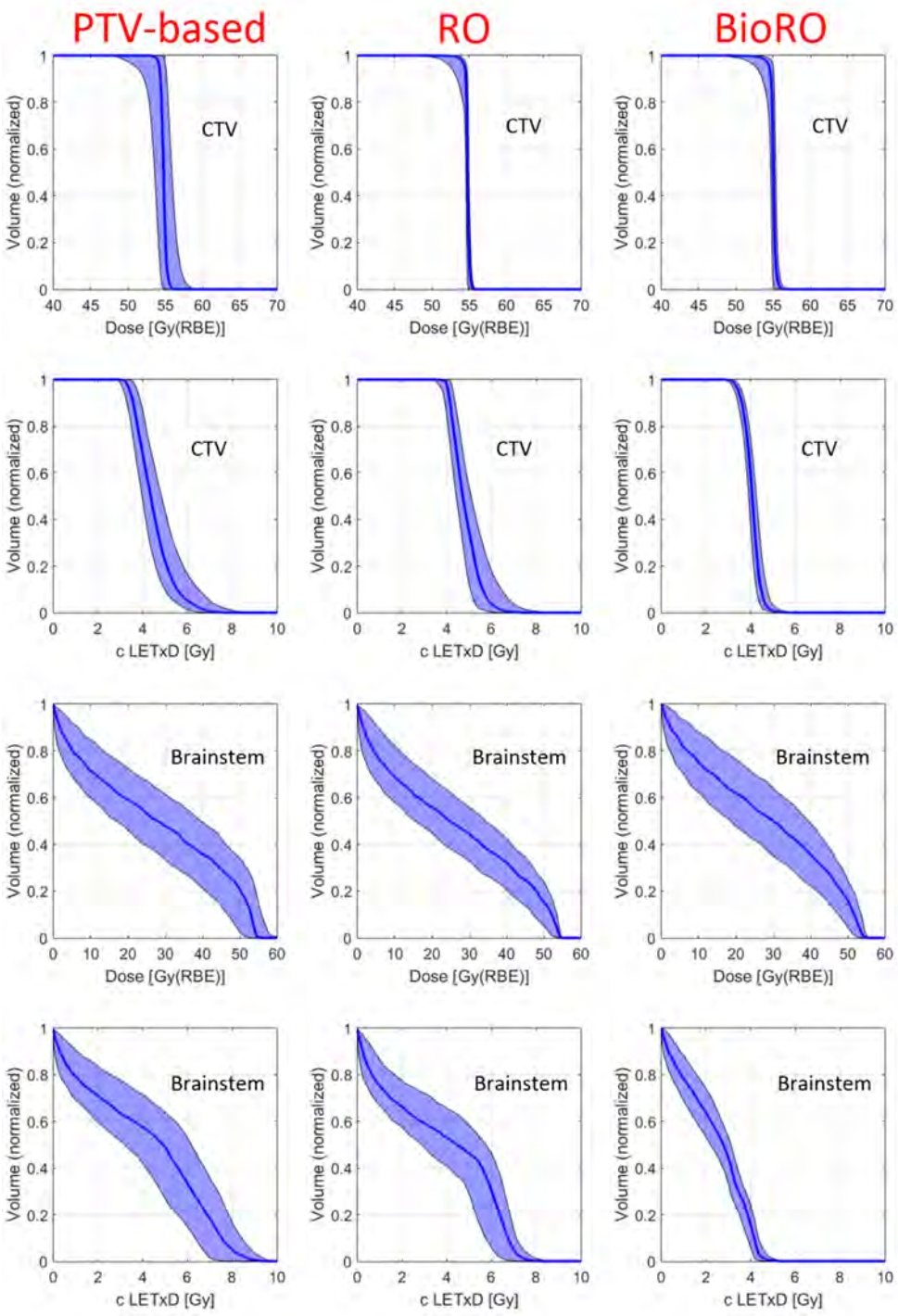

446

447 Figure 1. Dose-volume histograms (DVHs) and c LETxD-volume histograms of the clinical target volume

448 (CTV) and the brainstem for three IMPT plans in a brain tumor patient case: PTV-based optimization,

449 robust optimization (RO), and biological effect-based RO (BioRO). The bands were constructed on the

450 basis of nine uncertainty scenarios with various range shifts and setup errors. The bold lines indicate the
451 nominal distributions.
452

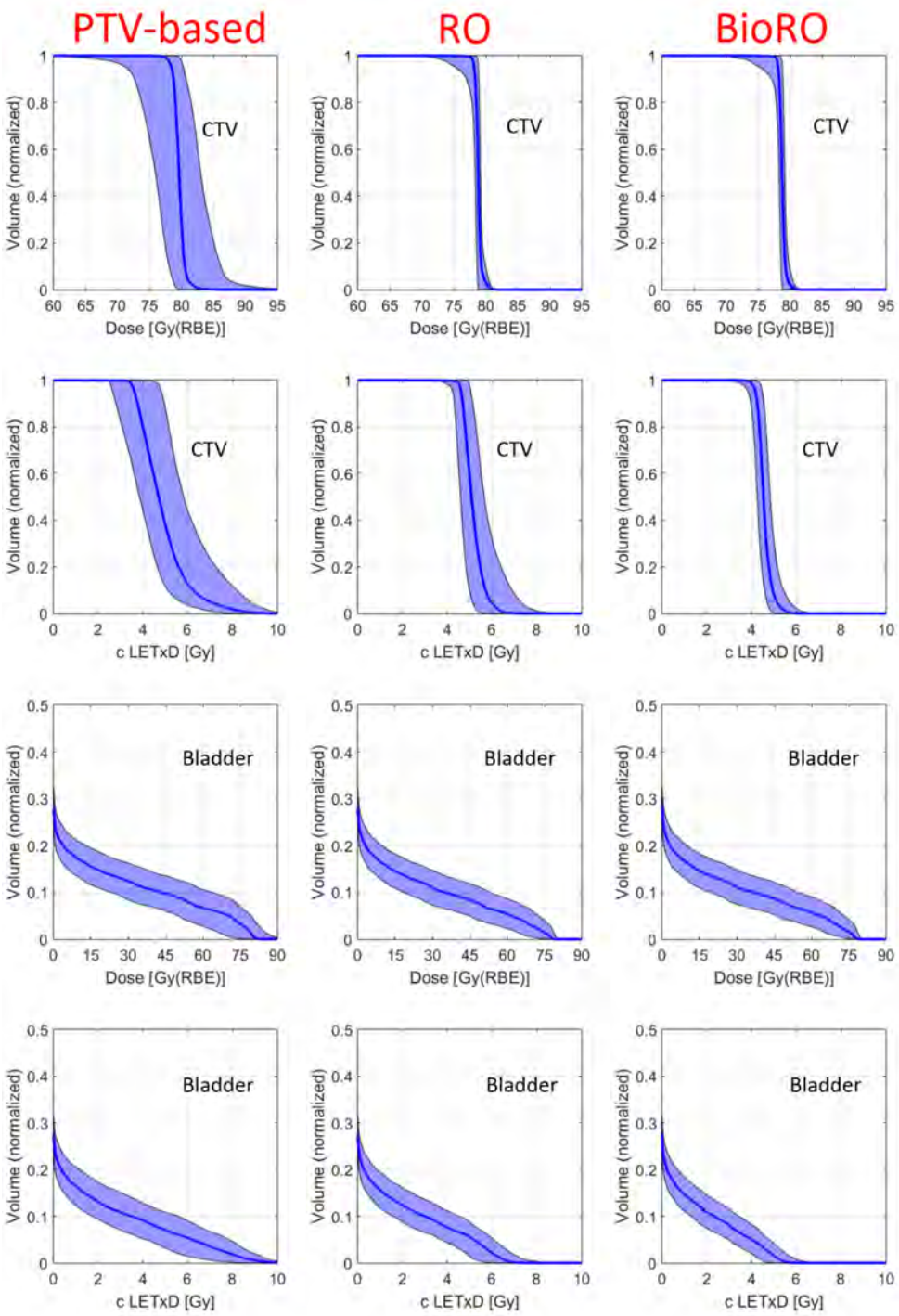

453

454 Figure 2. Dose-volume histograms (DVHs) and c LETxD-volume histograms of the clinical target volume

455 (CTV) and the bladder for three IMPT plans in a prostate tumor patient case: PTV-based optimization,

456 robust optimization (RO), and biological effect-based RO (BioRO). The bands were constructed on the

457 basis of nine uncertainty scenarios with various range shifts and setup errors. The bold lines indicate the
458 nominal distributions.
459

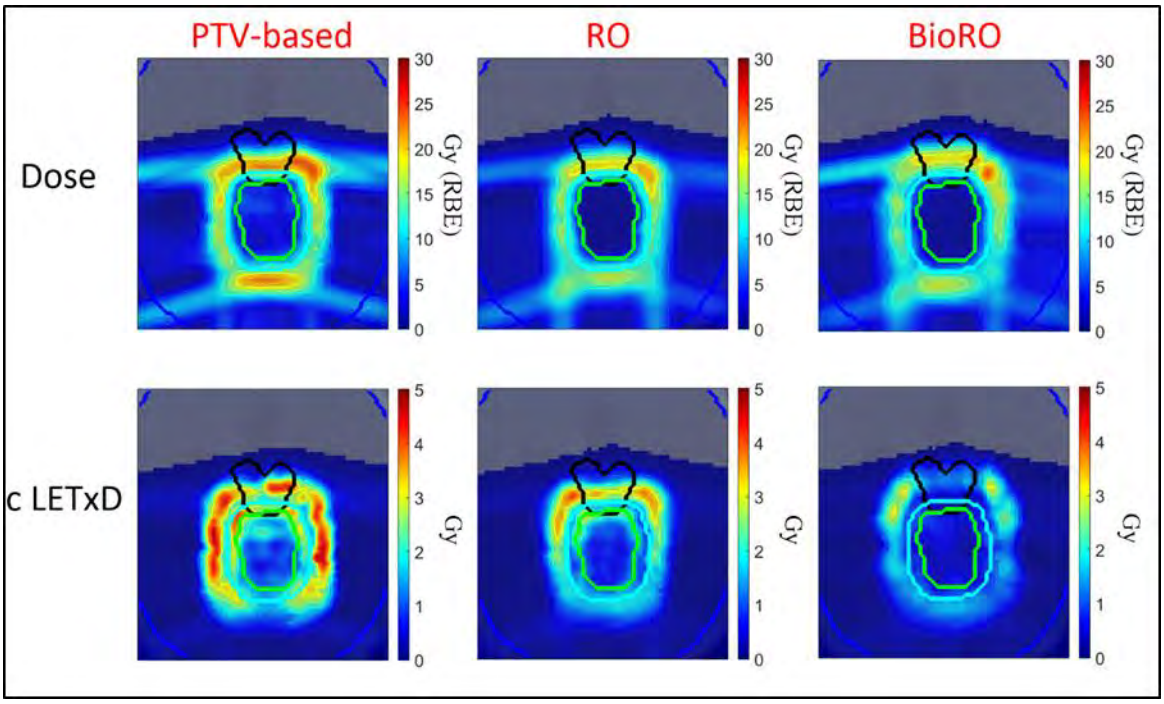

Figure 3. Distribution of differences between the maximum and minimum values in each voxel PTV-based, robust optimization (RO), and biological effect-based RO (BioRO) plans for the brain tumor patient case. The top row shows the difference distributions for dose (based on a constant RBE of 1.1). The bottom row shows difference distributions for LET weighted dose (LETxD) (scaled by c =0.04 µm/keV). The green and black contours indicate the clinical target volume (CTV) and brainstem, respectively.

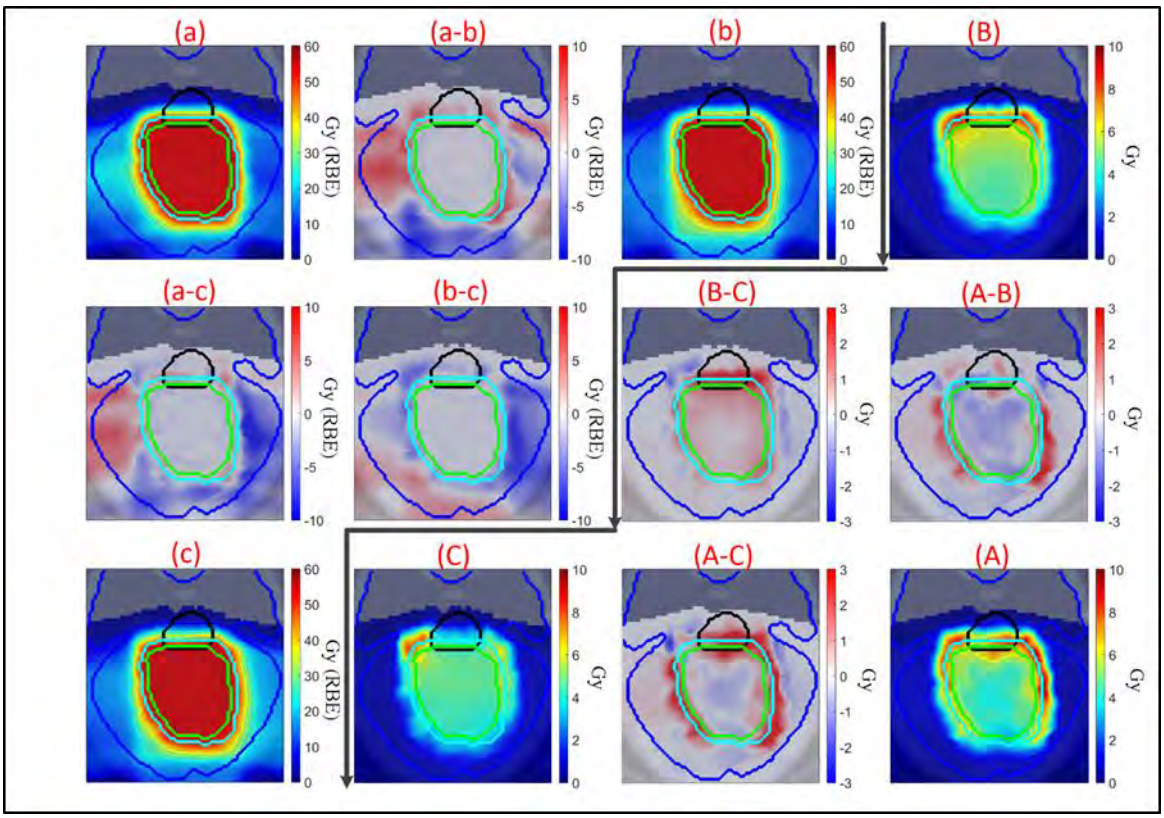

Figure 4. Comparison of PTV-based, robust optimization (RO), and biological effect-based RO (BioRO) plans for the brain tumor patient case. Panels (a), (b), and (c) show dose distributions (based on a constant RBE of 1.1) for the nominal scenario for PTV-based, RO, and BioRO plans , respectively. Panels (A), (B), and (C) show LET-weighted dose (LETxD) distributions (scaled by c = 0.04µm/keV) for the nominal scenario for PTV-based, RO, and BioRO plans, respectively. Panel (a – b) illustrates the absolute difference of (a) and (b), calculated by subtracting the value in (b) from the value in (a) for each voxel. The same method was applied for (a-c), (b-c), (A-B), (A-C), and (B-C). The green and black contours indicate the clinical target volume (CTV) and brainstem, respectively.

Appendix A. Dose-volume histograms and c LETxD-volume histograms in the CTV and larynx for plans optimized by PTV-based, RO and BioRO for the head & neck tumor case.

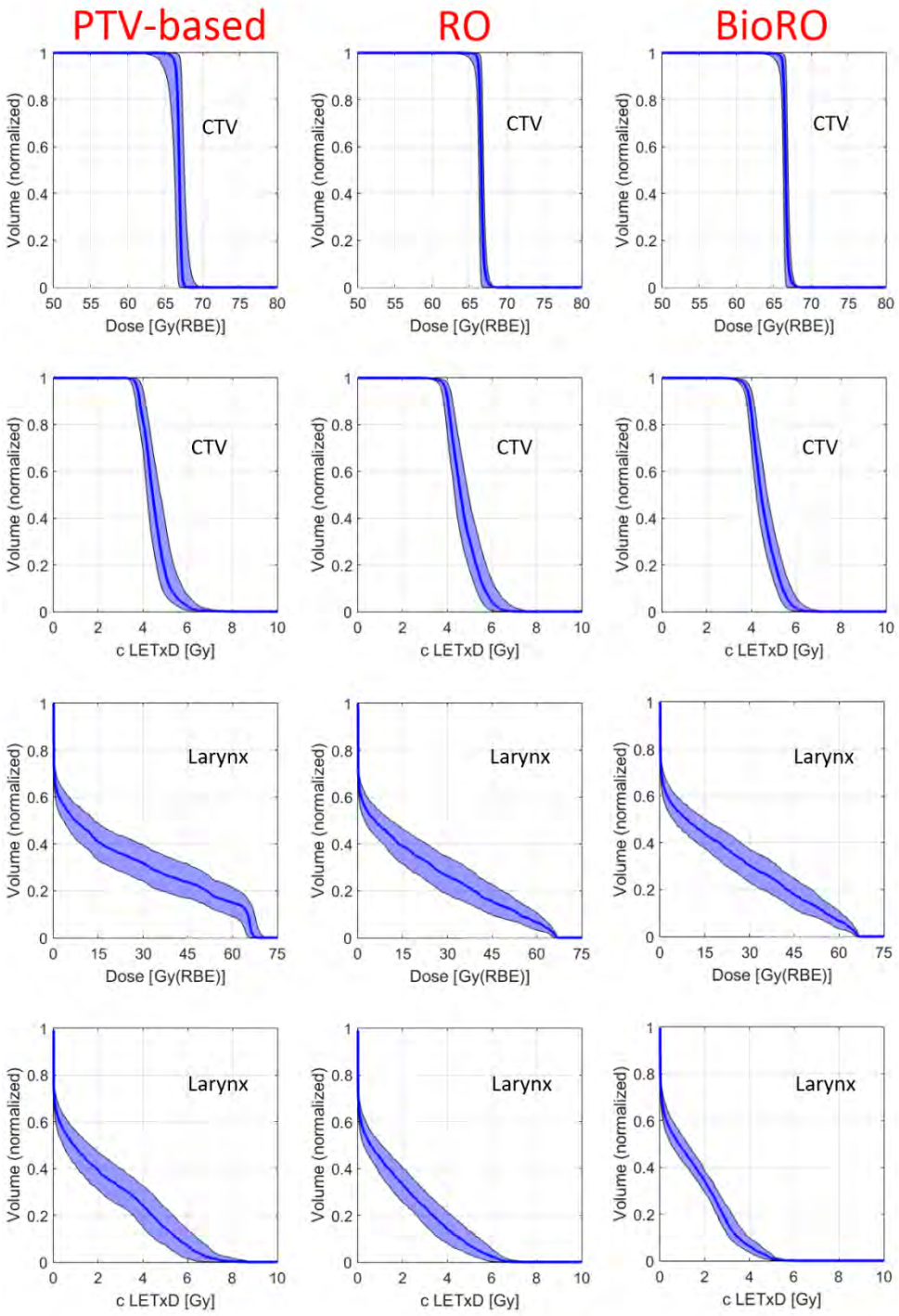

Figure A1. Dose-volume histograms (DVHs) and c LETxD-volume histograms of the clinical target volume (CTV) and the larynx for three IMPT plans in a head & neck tumor patient case: PTV-based optimization, robust optimization (RO), and biological effect-based RO (BioRO). The bands were constructed on the basis of nine uncertainty scenarios with various range shifts and setup errors. The bold lines indicate the nominal distributions.

Appendix B. Dose-volume histograms and c LETxD-volume histograms in the parotid (right & left) for plans optimized by PTV-based, RO and BioRO for a head & neck tumor case.

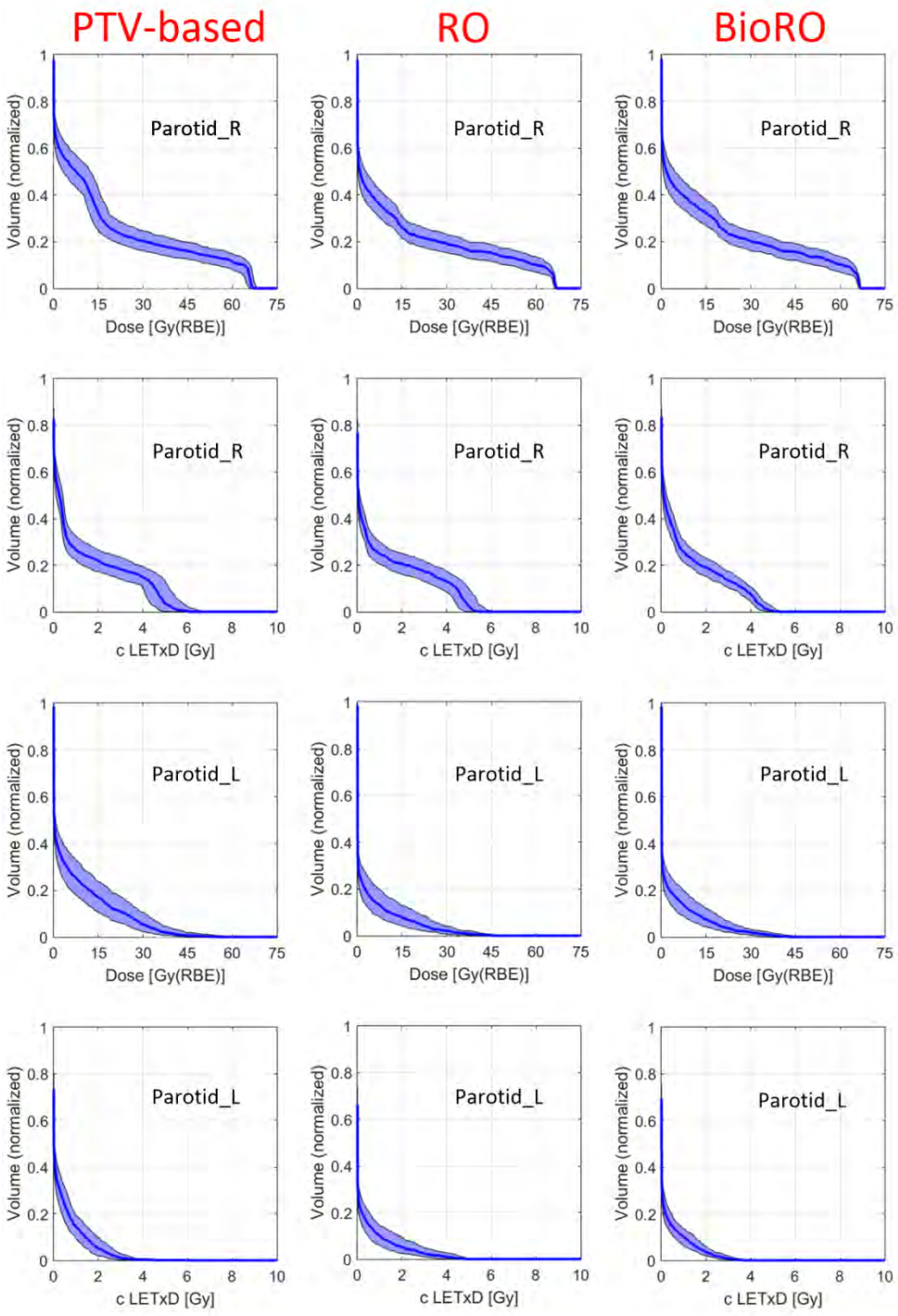

Figure B1. Dose-volume histograms (DVHs) and c LETxD-volume histograms of the parotid (right & left) for three IMPT plans in a head & neck tumor patient case: PTV-based optimization, robust optimization (RO), and biological effect-based RO (BioRO). The bands were constructed on the basis of nine uncertainty scenarios with various range shifts and setup errors. The bold lines indicate the nominal distributions.